AD-A173 710 AN ADAPTIVE NONCOHERENT PROCESSOR FOR MULTI-CHANNEL RADARS(U) COMMUNICATIONS RESEARCH CENTRE OTTAWA (ONTARIO) R W HERRING ET AL JAN 84 CRC-1369 1/1

UNCLASSIFIED F/G 17/9 NL

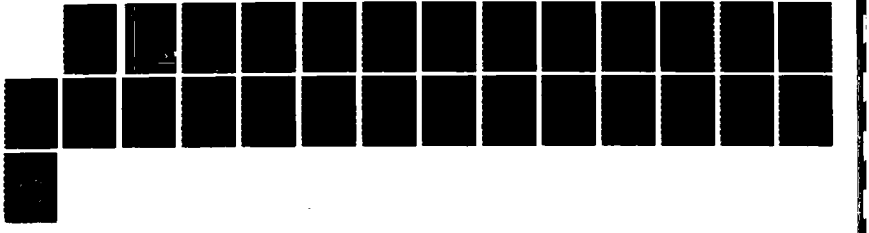

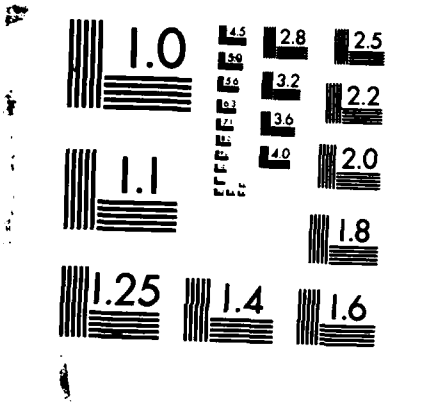

Communications Research Centre

AN ADAPTIVE NONCOHERENT PROCESSOR FOR MULTI-CHANNEL RADARS

by

R.W. Herring, R.M. Turner and E.K.L. Hung

This work was sponsored by the Department of National Defence, Research and Development Branch under Project No. 32C85.

CRC REPORT NO. 1369
OTTAWA, JANUARY 1984

Government of Canada
Department of Communications

Gouvernement du Canada
Ministère des Communications

Canada

COMMUNICATIONS RESEARCH CENTRE

DEPARTMENT OF COMMUNICATIONS
CANADA

AN ADAPTIVE NONCOHERENT PROCESSOR FOR MULTI-CHANNEL RADARS

by

R.W. Herring, R.M. Turner and E.K.L. Hung

(Radar and Communications Technology Branch)

CRC REPORT NO. 1369

January 1984
OTTAWA

This work was sponsored by the Department of National Defence, Research and Development Branch under Project No. 33C85.

TABLE OF CONTENTS

		Page
	ABSTRACT	1
1.	INTRODUCTION	1
2.	SYSTEM DESCRIPTION	2
	2.1 Gain Estimation	2
	2.2 Threshold Estimation	4
3.	SYSTEM PERFORMANCE	7
	3.1 Performance of ANCP Systems in a Known Noise Environment	8
	3.1.1 Optimum Gain Function	8
	3.1.2 Inverse Noise-Power Gain Function	8
	3.2 Performance of ANCP Systems which Estimate their Noise Environment	11
4.	SUMMARY AND RECOMMENDATIONS	11
	ACKNOWLEDGEMENTS	13
	REFERENCES	13
	APPENDIX A Derivation of the Optimum Gain Function	15
	APPENDIX B Mathematical Details	16

AN ADAPTIVE NONCOHERENT PROCESSOR FOR MULTI-CHANNEL RADARS

by

Robert W. Herring
Ross M. Turner
Eric K.L. Hung

ABSTRACT

An adaptive noncoherent processor (ANCP) system, intended as an ECCM for multi-channel (e.g., frequency agile) radars operating in a jamming environment, is described. The ANCP system operates by estimating the noise power in each active channel of the radar, adaptively adjusting the channel gain, and then noncoherently combining the outputs of the channels before executing a single target present/not-present threshold detection.

An example of the theoretical performance of an ANCP system in the presence of white-noise jamming with Gaussian statistics is presented. It is shown that a practical system performs within 3 dB or better of an ideal optimum system using prior knowlege of the jamming and target powers. The report concludes with appendices outlining the mathematical techniques for computing these results.

1. INTRODUCTION

Multi-channel radars, such as frequency-agile radars or netted radars, are used for their enhanced target-detection and ECCM capabilities. The purpose of this report is to describe the theoretical target-detection and anti-jam properties of an adaptive noncoherent processor (ANCP) which produces for each range-doppler cell a single target present/non-present decision base on the combined outputs of the multiple channels. It is also shown how to estimate these properties analytically.

The ANCP operates by estimating the noise power present in each channel and then using this estimated noise level to adjust the gain of the channel according to some predetermined algorithm. This approach is particularly useful when the noise levels differ in the various channels. Such is the case, for example, when a frequency-agile radar is subject to wide-band barrage jamming in its sidelobes, since the frequency dependence of the detailed sidelobe structure can induce significant channel-to-channel variation in the observed jammer noise.

In this report it is assumed that the target statistics on a channel-to-channel basis are Rayleigh or Swerling's Case 2, and that the noise in each channel is white with Gaussian statistics. The adaptive gain algorithms are derived under these assumptions. It turns out that for practical implementation the ANCP reduces to a form of the ratio detector described by Trunk [1-3]. The main differences between the present work and that of Trunk are in the derivation of and justification for the choice of the channel-to-channel gain adjustment algorithm, and in the techniques used to estimate the target detection and anti-jam performance.

Section 2 contains a description of the operation of a generalized ANCP system in the presence of white noise jamming. It begins with the derivation of the optimum adaptive gain function, where it is assumed that prior knowledge of the average noise levels is available. It is shown that considerable simplification in implementation occurs if the ANCP system is optimized for large-amplitude echoes, in which case it becomes a ratio detector. Section 3 describes and compares the theretically expected performance of three ANCP systems. The first is the optimum ANCP system with prior knowledge of its jamming environment. The second is a simplified sub-optimum ANCP system with prior knowledge of its jamming environment. The third is a sub-optimum ANCP system which adapts itself to the observed jamming environment. Only this third system is easily realized; the first two serve as benchmarks against which to measure the cost of simplifying the system's operation and the cost of estimating the noise environment directly. Section 4 summarizes these results and makes recommendations for further investigations. This report also includes an Appendix outlining the mathematical procedures followed in computing the results of Section 3.

2. SYSTEM DESCRIPTION

Fig. 1 shows an ANCP system suitable for a step-scan frequency-agile radar with M channels. (For clarity, the processing for only a single range cell has been included). The system operates as follows: The signal in each carrier-doppler channel (m,k) is square-law detected to yield the sample variate $\hat{t}_M(k)$ defined by Eqn. (1):

$$\hat{t}_M(k) = \sum_{m=1}^{M} G(M,k)\ \hat{t}(m,k) \quad . \tag{1}$$

$\hat{t}_M(k)$ is then compared with an adaptively computed threshold, $\hat{T}_M(k)$, to decide whether or not a target is present in the k'th doppler channel of the test range cell. (The circumflex denotes the sample value of a stochastic quantity.)

2.1 Gain Estimation

In Appendix A it is shown that for white noise jamming with Gaussian statistics and Swerling's Model 2 (Rayleigh) channel-to-channel target statistics, the optimum value for the adaptive gain for channel (m,k), $G_{opt}(m,k)$, is given by,

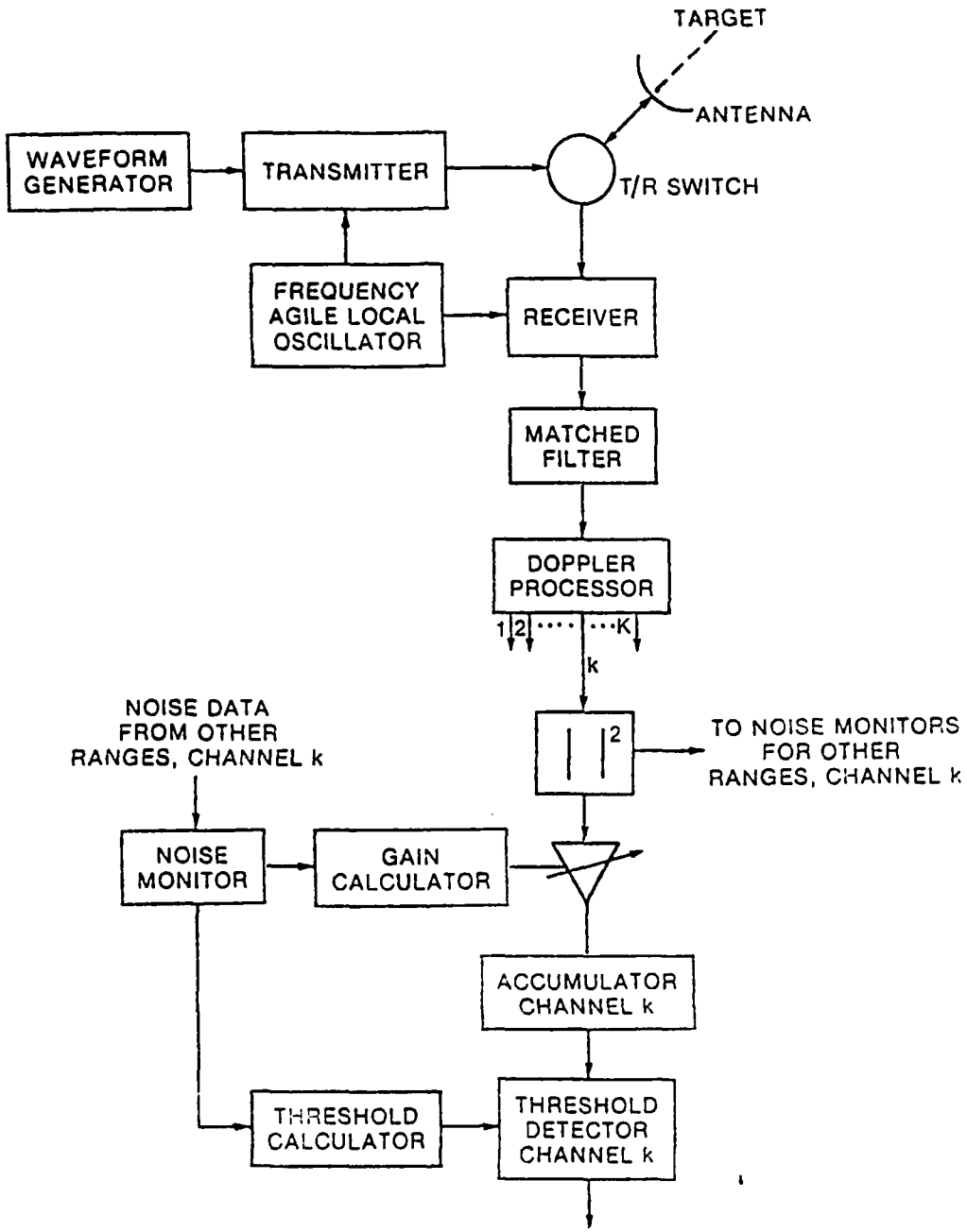

Figure 1 - **Frequency-Agile Implementation of an ANCP System.**

$$G_{opt}(m,k) = \frac{1+S_o}{[1+X(m,k)][1+X(m,k)+S_o]} \tag{2}$$

where unit internal white noise power spectral density (PSD) has been assumed, X(m,k) is the external white noise PSD due to jamming and is assumed to be known exactly, and S_o is the particular average target signal energy to quiescent internal noise PSD ratio (SNR) to which the system has been matched.

One purpose of this report is to investigate the effect of replacing [1+X(m,k)] in Eqn. (2) with estimated values based on observed samples of the total internal plus external noise. An unbiased estimate for [1+X(m,k)] is given by:

$$\hat{Y}_L(m,k) = \frac{1}{L} \sum_{\ell=1}^{L} y_\ell(m,k) \tag{3}$$

where the $\hat{y}_\ell(mk)$'s are square-law detected noise samples drawn from nearby range bins which are assumed not to contain target signals, and the subscript L denotes an L-sample estimate. Under the assumption of Gaussian statistics, $Y_L(m,k)$ has a Chi-squared distribution with 2L degrees of freedom. A suitable system for implementing Eqn. (3) is shown in Fig. 2.

An estimate of $G_{opt}(m,k)$ is given by:

$$\hat{G}_{opt}(m,k) = \frac{1+S_o}{\hat{Y}_L(m,k)\ [\hat{Y}_L(m,k)+S_o]} \tag{4}$$

Equation (4) can be substituted into Eqn. (1) to define the operation of an optimum ANCP system.

2.2 Threshold Estimation

For any adaptive detection scheme it is necessary to set the detection threshold on the basis of the observed noise and interference levels. It will now be shown how to do this for an ANCP system.

In general, the threshold level is set on the basis of providing an acceptable rate of false-alarm threshold crossings when there is known to be no target present. Ideally, this threshold level can be estimated as a simple function of the observed noise levels. The simplest possible estimator for the adaptive threshold $\hat{T}_M(k)$ for an ANCP system would be given by:

$$\hat{T}_M(k) = \gamma \hat{Z}_M(k) \tag{5}$$

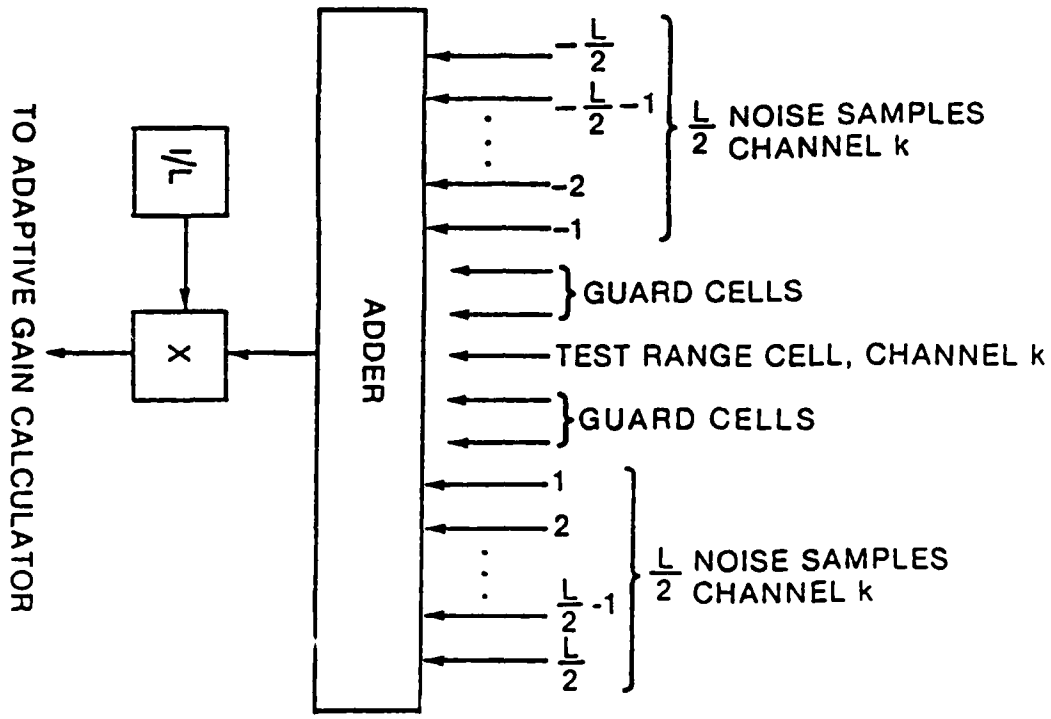

Figure 2 - **Noise Monitor, Doppler Channel k**

where

$$\hat{Z}_M(k) = \sum_{m=1}^{M} \hat{G}(m,k)\ \hat{Y}_L(m,k) \qquad (6)$$

and γ is a constant to be determined on the basis of the statistical distribution of $\hat{Z}_M(k)$. $\hat{Z}_M(k)$ is an estimate of the adaptively combined noise powers of the threshold detector.

A fundamental difficulty in using the estimated optimum gain function in practice is revealed if Eqn. (6) is further analyzed by considering the contribution, $\hat{z}(m,k)$, of a single channel to the sum in Eqn. (6), where

$$\hat{z}(m,k) = \hat{G}(m,k)\ \hat{Y}_L(m,k) \tag{7}$$

If the optimum gain function of Eqn. (4) is substituted into Eqn. (7), then,

$$\hat{z}_{opt}(m,k) = \frac{1+S_o}{\hat{Y}_L(m,k) + S_o} \tag{8}$$

and it is clear that $\hat{Z}_{M,opt}(K)$ as defined by Eqns. (7) and (6) is the sum of M non-linearly transformed Chi-squared distributed variates, each with 2L degrees of freedom and potentially different means.

It seems apparent that the statistical distribution of $\hat{Z}_{M,opt}(k)$ is not easily calculable, nor is it likely that the desirable simple linear relationship between the threshold setting and the noise-only output variate as defined by Eqn. (5) is valid. However, this challenging problem is obviated by optimizing for very large SNRs, which results in an easily implemented system with sub-optimum performance.

In the limit $S_o \to \infty$, Eqn. (8) reduces to

$$\hat{z}_\infty(m,k) = 1 \tag{9}$$

so that, according to Eqn. (5), the threshold $T_{M,\infty}(k)$ is given by

$$T_{M,\infty}(k) = \gamma M \tag{10}$$

which is a constant independent of the observed external noise level. This result means that in principle an ANCP system using inverse noise weights gives constant false-alarm rate (CFAR) performance using a fixed threshold, because of the normalization of the M components of the test variate $t_M(k)$. In practice, this result means that the threshold can be set empirically and can be expected to be relatively stable, provided the assumption of Gaussian noise statistics is not badly violated. This remains as a point for experimental investigation.

Again in the limit $S_o \to \infty$, the gain function $G_\infty(m,k)$ is found from Eqn. (4) to be:

$$\hat{G}_\infty(m,k) = \frac{1}{\hat{Y}_L(m,k)} \tag{11}$$

which is simple to estimate and implement. For these compelling reasons,

the remainder of this report shall be concerned principally with the performance of the sub-optimum inverse-noise weighted implementation of the ANCP system, although results for the optimum system have been included as the ultimate standard of performance.

3. SYSTEM PERFORMANCE

In this section the theoretically expected detection and anti-jam performance of an ANCP system is investigated. The number of carrier frequencies, M, has arbitrarily been chosen to be 10.

Section 3.1 contains discussions of the theoretical performance of ANCP systems when the external noise powers are known exactly. Section 3.1.1 discusses the performance of a system using the optimum gain function. These discussions provide a basis for quantitative estimates of how much the system performance is degraded by the use of the sub-optimum inverse gain function.

Section 3.2 contains results of the theoretical analysis of the performance of 10-channel ANCP systems using inverse gains estimated using L=8, 16 and 32 samples of the external noise in each of the channels. Comparison of these results with those of Sections 3.1.1 and 3.1.2 allows estimation of the losses due to using sample observations of the ambient noise instead of prior knowledge.

In both Sections 3.1 and 3.2, the numerical results were computed using the characteristic function method of Bird [3]. In Section 3.1 the required characteristic functions are straightforward modifications of the well-known characteristic function of the Chi-squared distribution. In Section 3.2 matters were considerably more complicated. The mathematical details are contained in Appendix B.

In the following analyses these basic assumptions were made: The target echo amplitudes were assumed to be uncorrelated on a channel-to-channel basis, and the target echo amplitudes were assumed to have Swerling's Case 2 or Rayleigh statistics. It was assumed that the powers radiated at each carrier frequency were identical, so that the received echo decorrelation on a channel-to-channel basis was due solely to the target cross-section characteristics. (The effect of a systematic channel-to channel variation in target echo strength can be incorporated into the analysis, as pointed out in Appendix B.3.1. Such variations arise, for example, due to scanning modulation in rotating antenna radars.)

The system chosen for analysis had 10 channels (M=10) with a design false-alarm rate (FAR) of 10^{-6} and a probability of target detection (P_D) of 90 percent. The number of jammed channels, J, ranged from 0 to 10, and all the jammed channels were assumed to have the same enhanced noise power levels. The parameter chosen as a measure of system performance was S, the average received echo energy in a single channel. S was expressed in decibels above the unit internal white noise PSD of an unjammed channel.

3.1 Performance of ANCP Systems in a Known Noise Environment

3.1.1 Optimum Gain Function

Results for an ANCP system with perfect prior knowledge of its noise environment are shown in Fig. 3. The number of jammed channels, J, has been plotted along the horizontal axis and S, the single-channel average echo energy acquired to produce a P_D of 90 percent where the threshold has been set to maintain a FAR of 10^{-6}, has been plotted along the vertical axis. The system performance has been plotted as curves of S vs J for levels of internal plus external noise in the jammed channels ranging from 3 dB to 30 dB above the quiescent internal noise level of 0 dB. At each point on these curves, the value of S_o in the optimum gain function G_{opt} of Eqn. (2) was set equal to S. The values of S required by systems composed of M=1 to M=10 channels to maintain this same performance in the absence of jamming have also been indicated in this figure.

In Fig. 3 (and in the other performance curves to be discussed below), there are certain fixed points of interest. Specifically, these points correspond to the case of no jamming (J=0) and all channels jammed equally (J=10). In each of these cases the gains in all 10 channels become identical, regardless of the gain-setting algorithm used. (In the case of all channels jammed identically, S must be increased by the same number of dB as the noise level, in order to maintain the required P_D.) The effect of the choice of adaptive gain function is to control the shape of the curves joining these fixed points.

The important observations from Fig. 3 are that in the presence of jamming the optimum ANCP system performs at least as well as one having 10-J channels, and that the J jammed channels are more or less ignored by the system, according to how heavily they are jammed. In the case of "light" jamming (10 dB or less), the jammed channels continue to make a useful contribution to the summed output. In the case of "heavy" jamming (20 dB or more), the jammed channels are effectively "turned off" and ignored.

3.1.2 Inverse Noise-Power Gain Function

Results for an ANCP system which has perfect prior knowledge of its noise environment but which has been optimized for a fixed value of $S_o = \infty$ have been plotted in Fig. 4. It was shown in Section 2.2 that such a system has its channel gains set inversely proportional to the white-noise PSD in each channel. The required system performance of FAR = 10^{-6} and P_D = 90 percent is the same as that of Fig. 3.

Comparison of Figs. 3 and 4 shows the following. First, the values for S at the fixed points (J=0 and J=10) are the same for both figures, as discussed in Section 3.1.1. Second, for light jamming (10 dB or less), the inverse gain function gives performance within 0.4 dB of that of the optimum gain function.

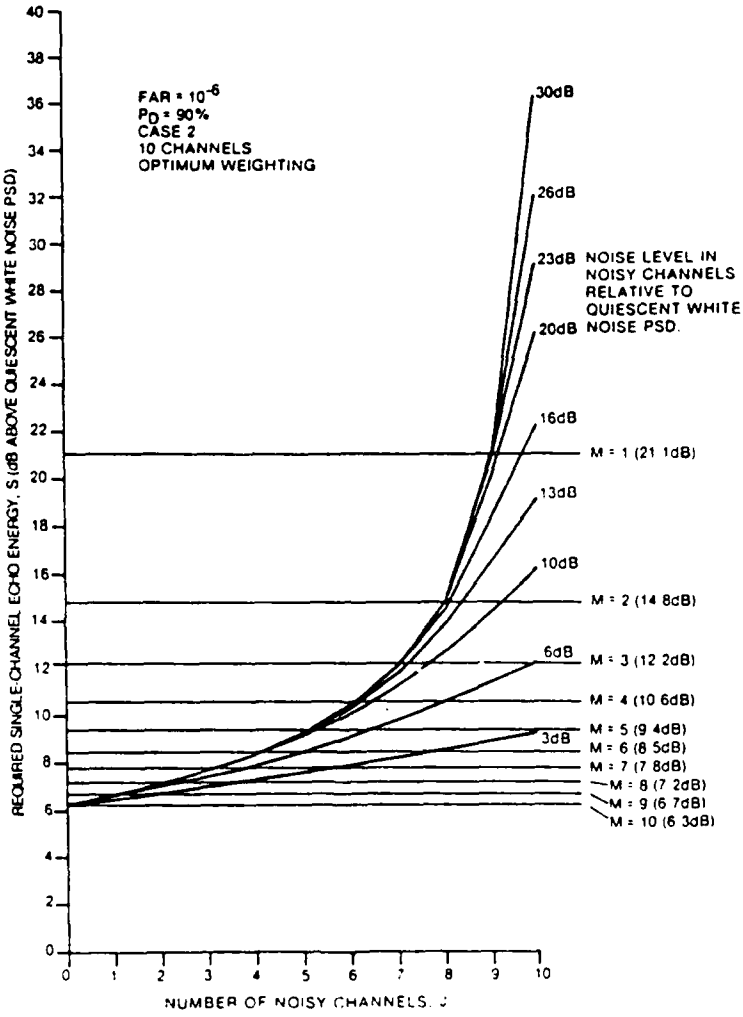

Figure - 3 **Required Average Single-Channel Echo Energy for a 10-Channel ANCP System Using a Priori Knowledge of the Noise Environment and an Optimum Gain Function.**

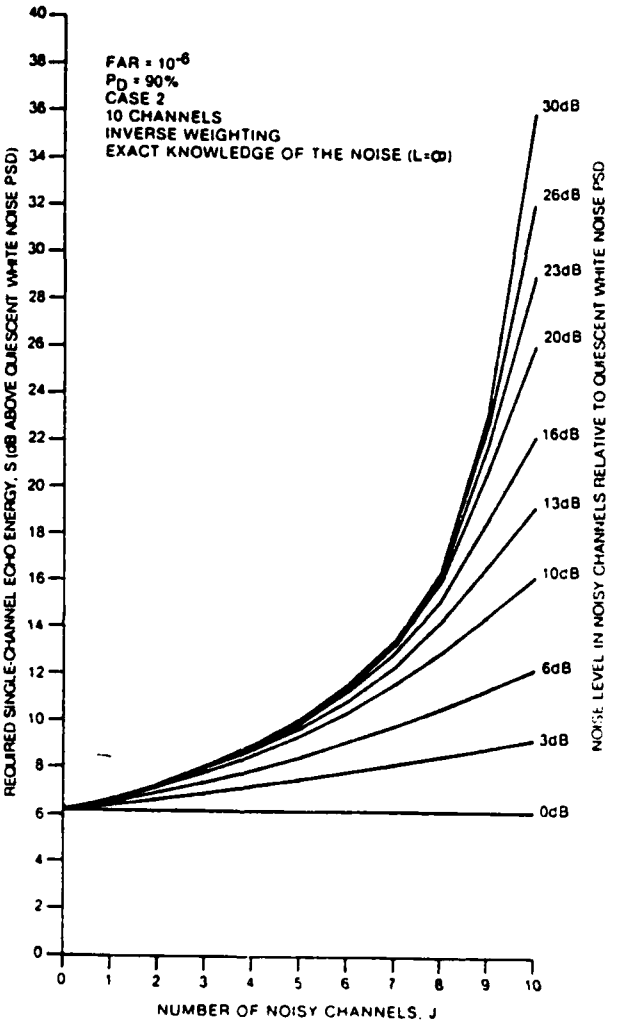

Figure 4 - **Required Average Single-Channel Echo Energy for a 10-Channel ANCP System Using a Priori Knowledge of the Noise Environment and the Inverse Noise Gain Function.**

For heavy jamming (20dB or greater) the performance of the inverse gain system is inferior by amounts ranging from 0.6 dB for J=5 to 2 dB for J=9. The reason for this is that under heavy jamming the outputs from the jammed channels are not suppressed or "turned off", but instead each channel contributes an average of one unit of noise to the accumulator, thereby degrading the SNR at the threshold detector. However, it is the presence of this constant noise power level at the threshold detector that leads to the simple fixed-threshold CFAR performance of this system. For the 10-channel system considered here, this CFAR performance costs 2 dB or less in terms of additional power required.

3.2 Performance of ANCP Systems which Estimate their Noise Environment

Results for an ANCP system which uses inverse noise gains and estimates its noise environment according to Eqn. (3) and an implementation of the scheme diagrammed in Fig. 2 are given in Fig. 5. The value of L, the number of noise observations per channel, was chosen to be 16. All other parameters were as before.

Comparison of Figs. 4 and 5 shows that the shapes of the characteristic curves are essentially identical, but that those of Fig. 5 are displaced upwards by a factor of about 1.0 dB. This factor of 1.0 dB is the loss incurred by not having exact knowlege of the white noise environment.

The cases for L=8 and L=32 were also investigated. For the case L=32, the estimation loss was about 0.4 dB; for the case L=8 it was about 3 dB. The implication is that for a 10-channel system, 16 noise samples per channel provide adequate information about the noise environment, while at the same time allowing rapid adaptation in a non-stationary noise environment.

4.0 SUMMARY AND RECOMMENDATIONS

An adaptive non-coherent processor (ANCP) system for use in multichannel radar ECCM applications has been described and its performance has been analyzed theoretically. Of the three forms of implementation analyzed, the first two took advantage of prior knowledge of the noise and jamming environment and thus are of academic interest only. However, they provided benchmark information in assessing the performance of the third implementation, which uses observations of the noise environment to adapt its operating characteristics. It was shown that for the particular system investigated, having 10 independent frequency channels, a false- alarm rate of 10^{-6} and a target detection probability of 90 percent, the increase in radiated power needed to compensate for both a non-optimum operating characteristic or adaptive gain function and a lack of prior knowledge of the jamming and noise environment was a modest 3 dB.

It is recommended that further work relevant to the ANCP systm be done in three general areas. The first is to compare the performance of the ANCP system with the performance of systems which perform threshold

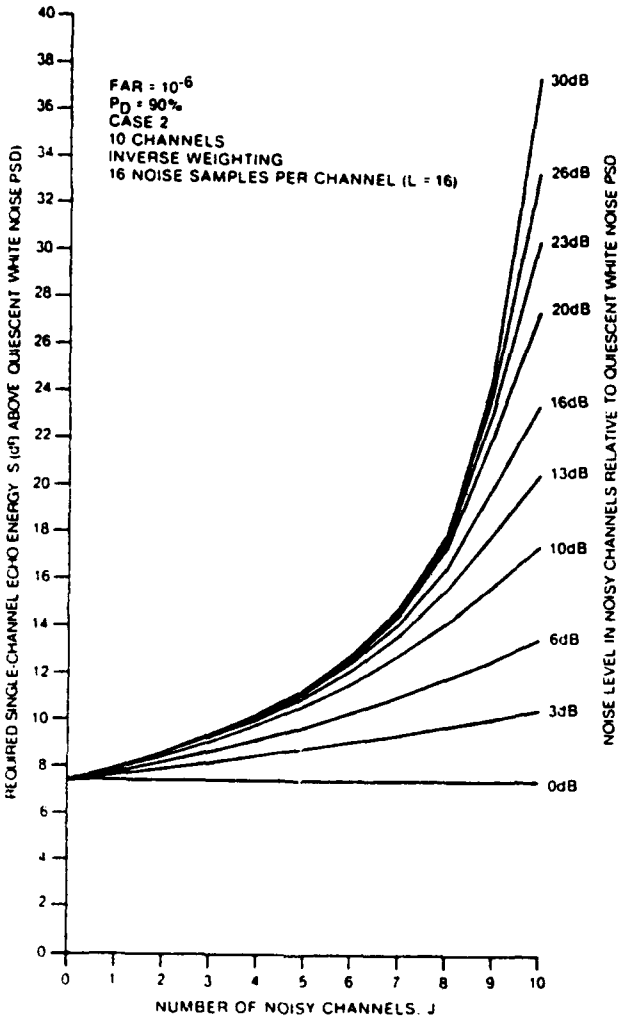

Figure 5 - **Required Average Single-Channel Echo Energy for a 10-Channel ANCP System Using 16 Samples of the Noise Environment in Each Channel to Estimate the Inverse Noise Gains.**

detection on their individual channels and then process the detector outputs in some manner. One such candidate system, which has already been investigated [4], is the M-channel system having a conventional adaptive-threshold CFAR detector in each of the M channels. The adaptive thresholds are set to maintain a desired output false-alarm rate and a target detection is declared when the threshold levels are exceeded in N or more channels. N must be selected to optimize system performance in some manner.

The second general area of investigation is to simulate the performance of an ANCP systm via software modelling. In this manner any undue sensitivity of system performance to the presence of forms of jamming other than white noise, such as, for example, blinking tone jammers or frequency-sweeping jammers, would be revealed.

The third general area of investigation, subject to favourable results being obtained for the first two, is to perform measurements using an actual radar system such as the CRC phased-array radar. Successful results for these experiments would indicate that development of an add-on processor for existing frequency-agile radar systems would be warranted.

ACKNOWLEDGEMENTS

The authors thank Dr. John S. Bird for assistance in the derivation of Appendix A. This work was supported by the Department of National Defence under Project 33C85.

REFERENCES

[1] G.V. Trunk, "Comparison of Detectors in the Presence of Sidelobe Jamming", Naval Research Laboratory, Washington, D.C. NRL Report 8449, 23 October 1983.

[2] G.V. Trunk, "Automatic Detectors for Frequency-Agile Radars", Naval Research Laboratory, Washington, D.C. NRL Report 8571, 23 April 1983.

[3] G.V. Trunk and P.K. Hughes, II, "Automatic Detectors for Frequency-Agile Radars", IEE Conf. Publ. No. 216, "Radar-82", 18-20 October 1982, pp. 464-468.

[4] R.W. Herring, R.M. Turner and E.K.L. Hung, "The Performance of a Multi-Channel N:M Detector Using CFAR Against White Noise Jamming", CRC Technical Note No. 719, 12 January 1984.

[5] J.S. Bird, "Calculating Detection Probabilities for Systems Employing Noncoherent Integration", IEEE Trans. Aerosp. Electron. Systems., Vol. AES-18, No. 4, July 1982, pp. 401-409.

[6] P. Swerling, "Probability of Detection for Fluctuating Targets", IRE Trans. Information Theory, Vol. IT-6, No. 2, April 1960, pp. 269-308.

[7] W. Gautschi and W.F. Cahill, "Exponential Integral and Related Functions". In "Handbook of Mathematical Functions", edited by M. Abramowitz and I. Stegun, New York: Dover Publications, Inc., 1968, Chapter 5, pp. 227-251.

[8] Y.L. Luke, "The Special Functions and Their Approximations". New York: Academic Press, 1969, Vol. 2, Table 23, pp. 325-327.

[9] F.L. Bauer, "Nonlinear Sequence Transformations". In "Approximation of Functions", Proceedings of the Symposium on Approximation of Functions, General Motors Research Laboratories, Warren, Michigan, 1964, edited by H.L. Garabedian. Amsterdam: Elsevier Publishing Company, 1965, pp. 134-151.

APPENDIX A

DERIVATION OF THE OPTIMUM GAIN FUNCTION

For Swerling's Case 2, the echoes and the noises are mutually uncorrelated within a channel, and the channels are also uncorrelated. Thus, for a two-channel ANCP, the covariance matrix for the k'th doppler channel is

$$[R_1] = \begin{bmatrix} 1+X(1,k)+S_o & 0 \\ 0 & 1+X(2,k)+S_o \end{bmatrix} \tag{A.1}$$

when a signal with energy S_o is present. If the signal is not present, then the covariance matrix is

$$[R_0] = \begin{bmatrix} 1+X(1,k) & 0 \\ 0 & 1+X(2,k) \end{bmatrix} \tag{A.2}$$

Let $[\psi] = [R_0]^{-1}-[R_1]^{-1}$ be the difference between the inverses of $[R_0]$ and $[R_1]$. Then, since both the echoes and noises have been assumed to have Gaussian amplitude distributions, the test statistic for making a Neyman-Pearson decision regarding signal presence or absence in the k'th doppler channel is

$$T_k = (r_1^* \; r_2^*) \; [\psi] \begin{pmatrix} r_1 \\ r_2 \end{pmatrix}$$

where r_1 and r_2 are the outputs of the ANCP doppler channels (1,k) and (2,k). Eqn. (A.3) can be rewritten as

$$T_k = \sum_{m+1}^{2} \frac{S_o}{[1+X(m,k)][1+X(m,k)+S_o} |r_m|^2 \tag{A.4}$$

Extension to more than two doppler channels is trivial.

A simple scaling change, replacing S_o by $(1+S_o)$ in the numerator of the fraction in Eqn. (A.4), gives Eqn. (2) for the optimum gain $G_{opt}(m,k)$. The only effect of the scale change is to give $G_{opt}(m,k)$ unit value when there is no external noise.

APPENDIX B

MATHEMATICAL DETAILS

B.1 INTRODUCTION

The numerical results of Section 3 were computed using the method of Bird [5]. This is a technique by which the cumulative probability distribution of the test statistic at the accumulator output can be obtained directly using a Fourier series and the characteristic function of the probability density distribution.

The purpose of this Appendix is to show the derivations of the required characteristic functions for the cases of prior knowledge and of direct observation of the noise environment, and to show how the two error parameters in Bird's technique are determined.

B.2 DEFINITIONS OF FUNDAMENTAL RESULTS

In order to proceed it is necessary to introduce some definitions and fundamental results. To begin, if $p(x)$ is a probability density distribution, then its characteristic function, $C(\omega)$, is defined as its Fourier transform:

$$C(\omega) = \int_0^\infty p(x)\, e^{-j\omega x} dx \qquad (B.1)$$

The cumulative probability distribution $P(T)$, i.e. the probability $PR\{x \leq T\}$, is defined as:

$$P(T) = \int_0^T p(x)\, dx \qquad (B.2)$$

so that if $p(x)$ corresponds to the distribution of the test variate at a threshold detector and T is the threshold, then $P(T)$ is the probability of correct dismissal for the case of target not present or the probability of missed detection for the case of target present.

Suppose now that a variable gain is introduced into the system, so that $p(x)$ is replaced by a conditional probability density distribution $p(y|G)$, where

$$y = Gx \quad . \qquad (B.3)$$

Further, let it be assumed that G is a stochastic variable with probability density distribution $p(G)$, and that x and G are statistically independent. It is desired to compute the characteristic function of the probability density distribution underlying $P(T)$, where now

$$P(T) = \int_0^\infty p(G) \int_0^T p(y|G)\, dy\, dG \tag{B.4a}$$

$$= \int_0^\infty p(G)\ \ P(T|G)\, dG \tag{B.4b}$$

The required probability density distribution is found by differentiating Eqn. (B.4b) with respect to T:

$$p(x) = \int_0^\infty p(G)\ p(x|G)\, dG \tag{B.5}$$

so that the required characteristic function can be found by applying Eqn. (B.1):

$$\overline{C}(\omega) = \int_0^\infty p(G)\ C(\omega|G)\, dG. \tag{B.6}$$

The overbar here denotes averaging over the gain distribution and

$$C(\omega|G) = \int_0^\infty p(x|G)\ e^{-j\omega x} dx \tag{B.7}$$

is the characteristic function corresponding to $P(x|G)$. This result is used in Sections B.2.1 and B.3.1.

B.2 Perfect Prior Knowledge of the Noise Environment

B.2.1 Derivation of the Characteristic Function

For the single-hit or single-channel case with Swerling Case 2 statistics, the characteristic function of the probability density function at the output of the square-law detector is given by:

$$C_1(\omega) = \frac{1}{1+j\omega[1+S]} \tag{B.8}$$

where S is the average target SNR and the average noise power has been normalized to unity ([6], Eqn. (III.8)).

If additional white noise, X(m,k), is added to the input signal, then the unit noise is replaced by 1+X(m,k) and the characteristic function for the single channel case becomes:

$$C_1(\omega) = \frac{1}{1+j\omega[1+X(m,k)+S]} \tag{B.9}$$

If a deterministic gain, G(m,k), is then incorporated into the channel, the characteristic function is further modified to become:

$$C_1(\omega|G) = \frac{1}{1+j\omega G(m,k)[1+X(m,k)+S]} \tag{B.10}$$

However, since the gain is deterministic, its probability density distribution is a Dirac delta function and from Eqn. (B.6),

$$\overline{C}_1(\omega) = C_1(\omega|G) \tag{B.11}$$

Since the channels are assumed to be statistically independent, the well-known convolution theorem of statistics can be invoked [5], so that the characteristic function for the test statistic composed of the sum of the M independent outputs of an M-channel system is given by:

$$C_{m,k}(\omega) = \prod_{m=1}^{M} \frac{1}{1+j\omega G(m,k)[1+X(m,k)+S]} \tag{B.12}$$

B.2.2 Bounding the Errors

It is clear from comparison of Eqn. (B.12) with Eqn. (24) of [4] that the expansion interval R for the Fourier series used in Bird's technique is, by analogy with Eqn. (31) of [5],

$$R = \ln(M/\epsilon_R) \sum_{m=1}^{M} G(m,k)[X(m,k)+S] \tag{B.13}$$

where ϵ_R is chosen as the largest error acceptable due to replacing the normally infinite upper limit of integration in Eqn. (B.1) with the large but finite value R. Appropriate selection of a value for R controls the first source of error in Bird's technique. Values of ϵ_R of FAR/100 and 10^{-6} were chosen when setting the threshold and computing P_D, respectively.

The second source of error arises due to truncating the infinite series which occurs in the discrete Fourier transform. Rather than following the complicated procedure of [5], the simple expedient of stopping when the magnitude of the terms being accumulated in the sum Eqn. (12) of [5] become smaller than $\epsilon_R/10$ was adopted. Experience has shown that this stopping rule produces reliable results for Swerling's Case 2, both when setting the threshold level T and when estimating P_D as a function of T and S.

B.3 Direct Observations of the Noise Environment

B.3.1 Derivation of the Characteristic Function

The required characteristic function can be derived directly from

Eqns. (B.6) and (B.10) and then applying the convolution theorem to derive a final result analogous to Eqn. (B.12).

To begin, a simplified notation will be introduced. In particular, indices and subscripts will be suppressed. Thus Eqn. (B.10) is rewritten as

$$\overline{C}(\omega|G) = \frac{1}{1+j\omega G[\overline{X}+S]} \tag{B.14}$$

where $\overline{X}$ is the average <u>total</u> (internal plus external) noise in the test range cell, and the gain G is a stochastic variable. The desired averaged characteristic function, $\overline{C}(\omega)$, is given by

$$\overline{C}(\omega) = \int_0^\infty \frac{p(G)}{1+j\omega G[\overline{X}+s]} \tag{B.15}$$

where p(G) is the probability density distribution of the stochastic gain function.

For the case of inverse noise gains, the gain function is given by Eqn. (11):

$$G = 1/Y \tag{B.16}$$

where

$$Y = \frac{1}{L} \sum_{\ell=1}^{L} y \tag{B.17}$$

is the sum of L Chi-squared variates, each with two degrees of freedom. Therefore, Y has a Chi-squared probability density distribution with 2L degrees of freedom.

Equation (B.15) can be rewritten in this case as

$$\overline{C}(\omega) = \int_0^\infty \frac{p(Y)}{1+j\omega[\overline{X}+S]/Y}\, dY \tag{B.18}$$

where

$$p(Y) = \frac{(L/\overline{Y})^L\, Y^{L-1}\, e^{-LY/\overline{Y}}}{(L-1)!} \tag{B.19}$$

is the density function and $\overline{Y}$ is the expected value of Y. If it is assumed that the noise in the test cell is statistically identical to the noise in the noise-observation cells, then

$$\overline{X} = \overline{Y} \quad . \tag{B.20}$$

All that remains is to substitute equations (B.19) and (B.20) into Eqn. (B.18) and to solve by repeated application of integration by parts. Doing so yields

$$\overline{C}(\omega) = \frac{1}{(L-1)!} \left\{ \sum_{\ell=0}^{L-1} (L-1-\ell)! \; (-jL\omega')^{\ell} \right.$$

$$\left. + \; (-jL\omega')^{L} \; e^{jl\omega'} \; E_1(jL\omega') \right\} \tag{B.21}$$

where

$$\omega' = \omega(1+S/\overline{Y}), \tag{B.22}$$

and in general

$$E_{n+1}(z) = \int_1^{\infty} \frac{e^{-zt}}{t^n} \, dt \tag{B.23}$$

is the exponential integral of order n ([7], Eqn. (5.1.4)).

Equation (B.21) can be further simplified by repeated application of Eqn. (5.1.14) of [5], i.e.,

$$E_{n+1}(Z) = \frac{1}{n} \left[e^{-z} - z \; E_n(Z) \right] \tag{B.24}$$

$$(n = 1,2,3,\ldots)$$

to get

$$\overline{C}(\omega) = L \; e^{jL\omega'} \; E_{L+1}(jL\omega') \tag{B.25}$$

where again ω' is given by Eqn. (B.22).

It is noted that the effects of systematic channel-to-channel variations in the received signal can be incorporated by appropriate selection of the value for S in Eqn. (B.22) for each channel component of the characteristic function.

B.3.2 Computation of the Characteristic Function

Unfortunately, the exponential integral with complex or purely imaginary argument and order greater than one seems not to have been a popular topic of research, and an extensive literature seach did not locate any numerical algorithms for its computation. Hence it became necessary to develop some techniques here.

It was found experimentally that the problem could be broken into two parts, according to whether $\omega'L$ was greater than or less than 18. For $\omega'L < 18$, it was found that, by using double-precision (72-bit or 18 decimal place) floating point arithmetic on a Honeywell CP-6 system, $C(\omega)$ could be computed to 12-digit accuracy directly from Eqn. (B.21). $E_1(jL\omega')$ was computed by noting that

$$e^{jL\omega'} E_1(jLw') = g(L\omega') - jf(L\omega') \tag{B.26}$$

where the auxiliary functions f(Z) and g(Z) are defined as:

$$f(Z) = \int_0^\infty \frac{\sin t}{t+Z}\, dt \tag{B.27}$$

and

$$g(Z) = \int_0^\infty \frac{\cos t}{t+Z}\, dt \tag{B.28}$$

from Eqns. (5.2.12) and (5.2.13) of [7]. f(Z) and y(Z) were computed using a Chebyshev polynomial expansion [8].

For $L\omega' \geq 18$, Eqn. (B.25) was used. From [7], Eqn. (5.1.51), it is noted the $E_n(Z)$ can be expanded in a divergent asymptotic series:

$$E_n(z) \sim \frac{e^{-z}}{z}\left\{1 - \frac{n}{z} + \frac{n(n+1)}{z^2} - \frac{n(n+1)(n+2)}{z^3} + \ldots\right\} \tag{B.29}$$

Substitution of Eqn. (B.29) into (B.25) and some algebraic manipulation yields

$$\overline{C}(\omega) \sim \frac{1}{j\omega'}\left\{1 + \frac{1+L^{-1}}{(-j\omega')} + \frac{(1+L^{-1})(1+2L)^{-1}}{(-j\omega')^2} + \frac{(1+L^{-1})(1+2L^{-1})(1+3L^{-1})}{(-j\omega')^3} + \ldots\right\} \tag{B.30}$$

as an asymptotic expansion for $\overline{C}(\omega)$.

It turns out that Eqn. (B.30) is compuationally useful, in spite of its divergence. A form of Stieltjes summation, known as the eta-algorithm [9], was applied to Eqn. (B.30) with a large measure of success. (Stieltjes summation is a technique for forcing convergence on a class of asymptotic expansions which are known to correspond to functions which have finite values). It was found necessary to apply the eta-algorithm twice for the case of values of $L\omega'$ in the lower range before convergence to 12-digit accuracy was achieved. Caution was advised in [9] regarding this procedure; however, here it appeared to work successfully.

Finally, as a reassuring note of consistency it is observed that in the limit $L\to\infty$, corresponding to perfect knowledge of the noise environment, Eqn. (B.30) reduces to:

$$\overline{C}(\omega) = \frac{1}{j\omega'} \sum_{n=0}^{\infty} (1-j\omega')^{-n} \tag{B.31a}$$

$$= \frac{(j\omega')^{-1}}{1+(j\omega')^{-1}} \tag{B.31b}$$

$$= \frac{1}{1+j\omega(\overline{Y}+S)/\overline{Y}} \tag{B.31c}$$

which is the same result as given by Eqn. (B.10) for the case of inverse noise gains and prior knowledge of the noise environment.

B.3.3 Bounding the Errors

In finding the value for the threshold setting, T, needed to give the specified FAR, the value of R was initially set to 5T, where T was a trial estimate, and a trial value of the FAR was determined. T and R were then adjusted iteratively until the specified FAR was achieved. Finally, stability of the result was confirmed by increasing R by an arbitrary factor of 2.3 and verifying that this did not affect the estimated value of the FAR by a relative change of more than 1 percent.

In computing P_D, the initial value for R was chosen to be the greater of either 5T or that value given by Eqn. (B.13) with $\epsilon_R = 10^{-5}$. R was then successively doubled until the computed value of P_D remained stable to 1 part in 10^5.

In both situations, setting T and determining P_D, the same stopping rule for terminating the summation was used; i.e. that the absolute magnitude of the last term in the truncated sum should be less than 0.1 times the required tolerance in the accuracy of the FAR and P_D estimates. Thus these magnitudes were 10^{-9} and 10^{-6}, respectively, for the two situations.

UNCLASSIFIED

Security Classification

DOCUMENT CONTROL DATA - R & D

(Security classification of title, body of abstract and indexing annotation must be entered when the overall document is classified)

1. ORIGINATING ACTIVITY
Defence Research Establishment Ottawa
Department of National Defence
Ottawa, Ontario, K1A 0Z4

2a. DOCUMENT SECURITY CLASSIFICATION
UNCLASSIFIED

2b. GROUP

3. DOCUMENT TITLE
AN ADAPTIVE NONCOHERENT PROCESSOR FOR MULTI-CHANNEL RADARS

4. DESCRIPTIVE NOTES (Type of report and inclusive dates)
CRC Report

5. AUTHOR(S) (Last name, first name, middle initial)
R.W. Herring, R.M. Turner and E.K.L. Hung

6. DOCUMENT DATE	7a. TOTAL NO. OF PAGES	7b. NO. OF REFS
January 1984	22	9

8a. PROJECT OR GRANT NO	9a. ORIGINATOR'S DOCUMENT NUMBER(S)
33C69	CRC Report No. 1369
8b. CONTRACT NO	9b. OTHER DOCUMENT NO.(S) (Any other numbers that may be assigned this document)

10. DISTRIBUTION STATEMENT
Unlimited

11. SUPPLEMENTARY NOTES	12. SPONSORING ACTIVITY
	DREO

13. ABSTRACT

An adaptive noncoherent processor (ANCP) system, intended as an ECCM for multi-channel (e.g., frequency agile) radars operating in a jamming environment, is described. The ANCP system operates by estimating the noise power in each active channel of the radar, adaptively adjusting the channel gain, and then noncoherently combining the outputs of the channels before executing a single target present/not-present threshold detection.

An example of the theoretical performance of an ANCP system in the presence of white-noise jamming with Gaussian statistics is presented. It is shown that a practical system performs within 3 dB or better of an ideal optimum system using prior knowlege of the jamming and target powers. The report concludes with appendices outlining the mathematical techniques for computing these results.

DSIS

END

12-86

DTIC